Inorg. Chem. **2005**, *44*, 3063–3069

New Materials Derived from Ybco: $CrSr_2RECu_2O_8$ (RE = La, Pr, Nd, Eu, Gd, Tb, Dy, Y, Ho, Er, Lu)

Rocío Ruiz-Bustos, Myriam H. Aguirre, and Miguel Á. Alario-Franco*

Laboratorio de Química del Estado Sólido, Departamento de Química Inorgánica, and Laboratorio Complutense de Altas Presiones, Facultad de Química, Universidad Complutense, 28040 Madrid, Spain

Received August 5, 2004

Eleven new oxides, derived from yttrium barium copper oxide by replacing the square-planar copper [Cu–O_4] of the basal plane of the triple perovskite-based structure with octahedral Cr^{IV}, have been prepared at high pressure and temperature. Their crystal structures have been determined, and their complex microstructure has been established by means of high-resolution electron microscopy and electron diffraction. The materials have a general formula of $CrSr_2RECu_2O_8$ (RE = La, Pr, Nd, Eu, Gd, Tb, Dy, Y, Ho, Er, and Lu); they are tetragonal, show the symmetry of space group *P*4/*mmm,* and do not appear to be superconducting.

Introduction

Most of the work dedicated to the search of high-temperature superconductors has relied upon the synthesis of new materials derived from $YBa_2Cu_3O_7$ and, in particular, upon the substitution of one of the copper atoms in the unit cell, specifically, the one located in the so-called charge reservoir layer (CRL).[1] In this way, a number of families have been obtained in which different elements have replaced the usual square-planar [Cu−O_4] units.[2] Examples of these can be found in a number of reviews.[3] Often, the geometry of the coordination polyhedron changes, such as in the *oxicarbonates*, where carbon seats in the center of a triangle, the *gallates* $GaSr_2RECu_2O_7$ (RE = La−Nd and Sm−Lu),[4] where gallium is located in a tetrahedron,[5] or the *ruthenates* $RuSr_2RECu_2O_8$, in which ruthenium is at the center of an octahedron.[6,7] In this last case, at room pressure, only the members corresponding to RE = Gd, Sm, and Eu can be made. However, the use of high pressure has proven very useful in this context,[8] and we have been able to prepare a number of new ruthenates.[9] These ruthenates appear to be rather unusual in that they seem to show the coexistence of superconductivity and magnetism, two collective properties that are commonly reputed to be incompatible,[10,11] and an important effort has recently been made to study these materials.[12,13] Interestingly enough, similar materials with niobium and tantalum[14,15] in the place of ruthenium do not show these properties. In an attempt to extend the knowledge of these materials having octahedra in the CRL, we have prepared a new family, $CrSr_2RECu_2O_8$, where, for the first time, Cr^{IV} is present in one of these cuprates. The presence of Cr^{VI} in the CRL has previously been shown, in combination with copper in, for example, $(Cu,Cr)Sr_2Ca_{n-1}Cu_nO_{2n+3+\delta}$.[16] On the other hand, Cr^{IV}, a relatively infrequent oxidation

* To whom correspondence should be addressed. E-mail: maaf@quim.ucm.es and http://www.ucm.es/info/labcoap/index.htm.

(1) Tokura, Y.; Takagi, H.; Uchida, S. *Nature* **1989**, *337*, 345. See also: Alario-Franco, M. Á. *Adv. Mater.* **1994**, *7*(2), 229.
(2) For a recent review, see: Mitchell, R. H.; *Perovskites: Modern and Ancient*; Almaz Press: Ontario, Canada, 2002; chapters 2 and 8.
(3) Poole, C.; Creswick, R. C.; Farach, H. *Handbook of Superconductivity*; Elsevier: Amsterdam, 1999; p 136.
(4) Vaughey, J. T.; Thiel, J. P.; Hasty, E. F.; Groenke, D. A.; Stern, C. L.; Poeppelmeier, K. R.; Dabrowski, B.; Hinks, D. G.; Mitchell, A. W. *Chem. Mater.* **1991**, *3*, 935.
(5) Ramírez-Castellanos, J.; Matsui, Y.; Takayama-Muromachi, E.; Isobe, M. *J. Solid State Chem.* **1996**, *123*, 378.
(6) Bauernfein, L.; Widder, W.; Braun, H. D. *Physica C* **1995**, *254*, 151.
(7) Felner, I.; Asaf, U.; Reich, S.; Tasabba, T. *Physica C* **1999**, *311*, 163.
(8) Takayama-Muromachi, E. *Chem. Mater.* **1998**, *10*, 2686.
(9) Ruiz-Bustos, R.; Gallardo-Amores, J. M.; Sáez-Puche, R.; Morán, E.; Alario-Franco, M. Á. *Physica C* **2002**, *382*, 395−400.
(10) *Topics in Current Physics*; Fisher, O., Maple, M. B., Eds.; Springer-Verlag: New York, 1985.
(11) Maple, M. B. *Physica B* **1995**, *215*, 110−126.
(12) Felner, I.; Asaf, U.; Ritter, F.; Klamut, P. W.; Dabrowski, B. *Physica C* **2001**, *368*, 364−365.
(13) McLaughlin, A. C.; Attfield, J. P. *Phys. Rev B: Solid State* **1999**, *60*, 14605.
(14) Greaves, C.; Slater, P. R. *Physica C* **1989**, *161*, 245.
(15) Vybornov, M.; Perthold, W.; Michsor, H.; Holubar, T.; Hilscher, G.; Rogl, P.; Fischer, P.; Davis, M. *Phys. Rev. B: Solid State* **1995**, *52*, 1389.
(16) Loureiro, S. M.; Matsui, Y.; Takayama-Muromachi, E. *Physica C* **1998**, *302*, 344.

10.1021/ic048929y CCC: $30.25
Published on Web 03/29/2005

state for chromium in oxides,[17] requires the use of high pressure and temperature to get stabilized. However, once formed, these new materials are stable to relatively high temperatures in air (~650 °C). We describe, in this manuscript, the synthesis, structure and microstructure characterization, and magnetic properties of the materials corresponding to RE = La, Pr, Nd, Eu, Gd, Tb, Dy, Y, Ho, Er, and Lu.

None of these new oxides appear to be superconducting. Hereafter, we will describe our work on the basis of the gadolinium compound because, in the case of the ruthenates, it is the one that has been the most thoroughly studied; references will, nevertheless, be made to the other family members, which are indeed qualitatively similar.

Experimental Section

The synthesis experiments were performed in a Belt-type apparatus. Corresponding stoichiometric amounts of $SrCuO_2$ (made by heating copper(II) oxide and strontium carbonate for 72 h at 1000 °C), CrO_2 (kindly made available by BASF, Ludwigshafen, Germany), and the corresponding rare earth oxide RE_2O_3 (kindly supplied by Rhone-Poulenc, France), which was decarbonized by heating it in air at 950 °C for 12 h, were placed in platinum containers and heated to 1300 °C under a pressure of 60−80 kbar, according to the equation

$$2SrCuO_2 + {}^1/_2RE_2O_3 + CrO_2 + {}^1/_4O_2 \rightarrow CrSr_2RECu_2O_8 \quad (1)$$

All of the samples have been characterized by means of X-ray powder diffraction performed in a Siemens D-500 diffractometer (Cu Kα source, Ni filter). All of the the patterns are similar to that previously observed for $RuSr_2GdCu_2O_8$, with which these compounds are isostructural, as stated below.

The diffraction patterns were refined with the Rietveld procedure following the GSAS program.[18] As a starting model, we used the structure previously reported by McLaughlin et al. for $RuSr_2GdCu_2O_8$,[19] with which the materials appear to be isostructural. The *average* crystal structure of $CrSr_2GdCu_2O_8$ is tetragonal and shows the symmetry of space group *P*4/*mmm*. Backgrounds were fitted using a linear interpolation, and peak shapes were modeled by a pseudo-Voight function.

The sample composition was checked by energy-dispersive spectrometry (EDS; Link Pentafet 5947 Model, Oxford Microanalysis Group) and transmission electron microscopy (JEOL JEM FX2000) by in situ observations. High-resolution transmission electron microscopy and selected area electron diffraction were performed on a JEOL JEM 3000F−Field Emission Gun microscope.

Magnetic properties were measured with a Quantum Design MPMS-XL SQUID magnetometer. The temperature dependence of the magnetic susceptibility was measured under both field-cooled and zero-field-cooled conditions under an applied magnetic field of H =100 Oe in the temperature range T = 2−300 K.

Results and Discussion

Analytical Results. Composition analysis, as given by EDS, confirmed the nominal composition: $CrSr_2GdCu_2O_8$.

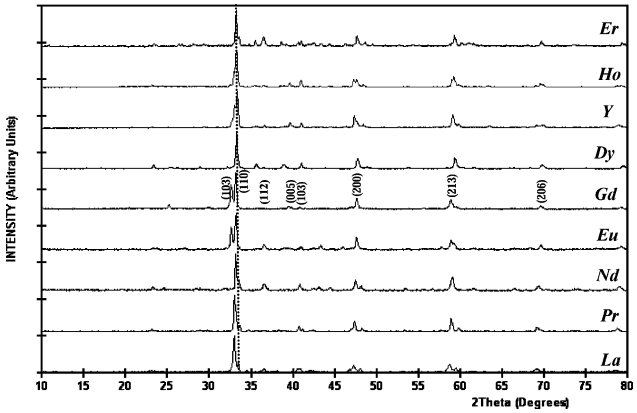

Figure 1. X-ray diffraction patterns for different members of the family $CrSr_2RECu_2O_8$.

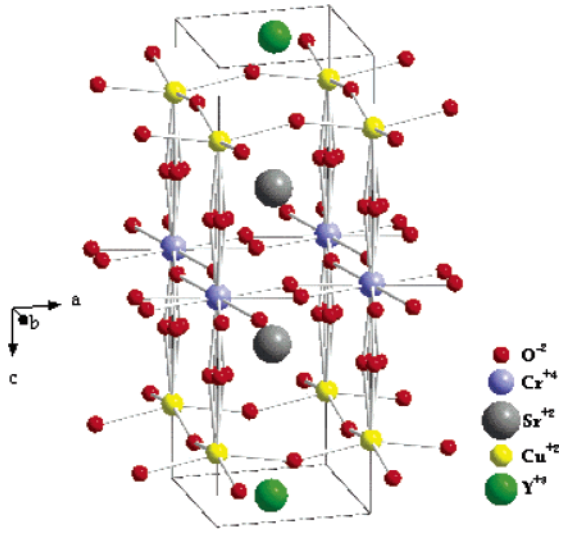

Figure 2. Crystal structure of $CrSr_2GdCu_2O_8$. Note the splitted O(1) and O(3) positions.

On the other hand, thermogravimetric analysis indicated that, in air, decomposition starts at ca. 650 °C, whereas in a nonoxidizing atmosphere, it initiates around 510 °C. In air, the weight loss after heating at 1000 °C is 0.81%, whereas in nitrogen it is 1.46%. The decomposition products are a mixture of different oxides of the metals (see below).

It is worth mentioning that chromium dioxide does decompose to Cr_2O_3 at a lower temperature of 430 °C in air.[20] This is an indication of the relatively low stability of Cr^{IV} in oxides, and this is the main reason for the need of high pressure in the synthesis of these chromates (having oxidation numbers of IV).

In this respect, the perovskite-based structure seems to be more favorable, by more than 200 °C, than the rutile one to stabilize Cr^{IV}. No indications were observed of oxygen under stoichiometry; in particular, the X-ray powder data taken on samples that were partly decomposed did not show any displacement of the diffraction peaks, just a decrease in the intensity of the original material's diffracted peaks, whereas those of the decomposition products did progressively appear. The main decomposition products, as suggested from the

(17) Cotton, F. A.; Wilkinson, G.; Gauss, P. L. *Basic Inorganic Chemistry*; Wiley & Sons: New York, 1995; p 600.
(18) Larson, A. C.; Von Dreele, R. B. *GSAS (General Structure Analysis System)*; Report LA-UR-86-748; Los Alamos National Laboratory: Los Alamos, NM, 1994.
(19) McLaughlin, A. C.; Zhou, W.; Attfield, J. P.; Fitch, A. N.; Tallon, J. L. *Phys. Rev. B: Solid State* **1999**, *60*, 7512.
(20) Alario-Franco, M. A.; Sing, K. S. W. *J. Therm. Anal.* **1972**, *4*, 47.

Table 1. Refined Cell Parameters, Agreement Factors, and Atomic Parameters for $CrSr_2GdCu_2O_8$

T (K)	a (Å)	c (Å)	V (Å)^3	R_{wp}	R_p	χ^2
298	3.8191(2)	11.4972(1)	167.693(2)	0.072	0.056	2.45

atom	site	x	y	z	U_{iso}(Å)^2	occupancy
Cr	1(*b*)	0	0	0.5	0.001(1)	1
Sr	2(*h*)	0.5	0.5	0.3092(2)	0.001(1)	1
Gd	1(*c*)	0.5	0.5	0	0.001(1)	1
Cu	2(*g*)	0	0	0.1611(1)	0.001(1)	1
O1	8(*s*)	0.0470(1)	0	0.3132(3)	0.003(2)	0.25
O2	4(*i*)	0	0.5	0.1312(1)	0.003(2)	1
O3	4(*o*)	0.1222(1)	0.5	0.5	0.003(2)	0.5

Table 2. Some Interatomic Distances and Angles in the $CrSr_2GdCu_2O_8$ Structure

distances (Å)		angles (deg)	
Cu−O(1) × 1	2.06(1)	O(1)−Cu−O(2)	91.07(4)
Cu−O(2) × 4	1.913(3)	O(2)−Cu−O(2)	89.12(3)
Cr−O(1) × 2	1.87(2)	O(2)−Cu−O(2)	166.32(2)
Cr−O(3) × 4	1.927(2)	O(1)−Cr−O(1)	180
Gd−O(2) × 8	2.432(2)	O(1)−Cr−O(3)	83.31(3)
Sr−O(1) × 2	2.582(5)	O(3)−Cr−O(3)	90
Sr−O(1) × 2	2.862(6)	O(3)−Cr−O(3)	180
Sr−O(2) × 4	2.765(2)	Cu−O(1)−Cr	168.61(6)
Sr−O(3) × 2	2.594(4)	Cu−O(2)−Cu	166.32(2)
Sr−O (3) × 2	3.201(7)	Cr−O(3)−Cr	151.52(4)

Table 3. Lattice Parameters of the Family $CrSr_2RECu_2O_8$ and Shannon and Prewitt Ionic Radii[26]

RE	a (Å)	c (Å)	c/a	V (Å^3)	R (Å)
La	3.86(1)	11.53(2)	2.99	171.79	1.160
Pr	3.843(4)	11.53(1)	3.00	170.28	1.126
Nd	3.835(2)	11.50(1)	3.00	169.13	1.109
Eu	3.825(2)	11.50(1)	3.01	168.25	1.066
Gd	3.819(1)	11.497(2)	3.01	167.68	1.053
Tb	3.817(1)	11.481(3)	3.01	167.26	1.040
Dy	3.815(1)	11.460(3)	3.00	166.79	1.027
Y	3.810(1)	11.468(2)	3.01	166.47	1.019
Ho	3.809(1)	11.463(3)	3.01	166.31	1.015
Er	3.803(1)	11.46(1)	3.01	165.74	1.004
Lu	3.794(3)	11.42(1)	3.01	164.38	0.977

powder data, were, in the case of $CrSr_2GdCu_2O_8$, Cr_2O_3, Gd_2O_3, $SrCrO_4$, and $SrCuO_2$.[21]

On the other hand, the corresponding ruthenates *obtained at high pressure* also decompose *at room temperature and pressure* in either an oxidizing or an inert atmosphere, their decomposition products being[21]

$$RuSr_2RECu_2O_8 \Rightarrow Sr_2RuREO_6 + 2CuO \qquad (2)$$

which is, in fact, the reverse of their synthesis reaction.[9]

Crystal Structure. Figure 1 shows the X-ray diffraction patterns for different members of the family.

We have performed Rietveld refinement fits to all of the X-ray data on the basis of a unit cell of the type $\sim a_p \times a_p \times 3a_p$, where a_p stands for the perovskite-type cell parameter; we use this as a basis because these materials show a 3-fold perovskite superstructure. The occupancy of each cation site was refined, as was the possible cross substitution between cations, for example, [Sr and Gd] and [Cu and Cr]; however, no disorder was found between these sites.[21]

Table 1 gives the refined cell and atomic parameters for $CrSr_2GdCu_2O_8$. It was observed, in the course of the refinement, that the oxygen ions in the equatorial plane of the [Cr−O_6] octahedra, that is, O(3), as well as the apical oxygens O(1), did show some disorder, as indicated by a rather high atomic displacement U factor, a feature also observed by McLaughlin et al in the isostructural $RuSr_2GdCu_2O_8$.[19] This is a common phenomenon in perovskites[2] and related materials, such as $La_{1/3}TaO_3$,[23] and was termed *incoherent octahedral tilting* by Amow and Greedan,[24] who also observed it in $K_2Nd_2Ti_3O_{10}$. Using a single isotropic factor and splitting the corresponding oxygen positions, as indicated in Table 1, solved the problem, as usual.[25] Figure 2 shows the structure where the splitted positions of the O(1) and O(3) oxygen atoms are indicated.

On the other hand, Table 2 gives some of the interatomic distances and angles observed in the structure of $CrSr_2GdCu_2O_8$.

The unit cell parameters characteristic of the different family members are plotted in Figure 3. Interestingly, whereas the a parameter, Figure 3a, is a linear function of the ionic radii of the rare earth ion in eight coordination,[26] the c parameter, Figure 3a, and, consequently, the unit cell volume, plotted in Figure 3b as a function of the cube of the rare earth ion in eight coordination, follow the lanthanide contraction. The c/a ratio remains practically constant at ∼3.0(1), Table 3. This is, indeed, the expected ideal value for a triple perovskite and seems to have consequences in the microstructure (see below).

The Metal−Oxygen Octahedra. It is worth mentioning that, although this structure is similar to the one[19,28] observed for $RuSr_2RECu_2O_8$, there are some interesting differences with respect to it. In the first instance, whereas the [Ru−O_6] octahedra are rather regular [cf. $d_{Ru-O(1)}$ = 1.987(10) Å and $d_{Ru-O(3)}$ = 1.9817(4) Å, giving a ratio d_1/d_3 = 1.003 for the Holmium compound $RuSr_2HoCu_2O_8$ obtained at high pressure[43]], the [Cr−O_6] octahedra are quite distorted [cf. $d_{Cr-O(1)}$ = 1.87(2) Å and $d_{Cr-O(3)}$ = 1.927(2) Å, with d_1/d_3 = 0.97 for $CrSr_2GdCu_2O_8$]. Also, in

(21) Ruiz-Bustos, R. Ph.D. Thesis, Universidad Complutense, Madrid, Spain, 2003. See also ref 9.
(22) Ruiz-Bustos, R.; Aguirre, M. H.; Alario-Franco, M. Á. *Mater. Res. Soc. Symp. Proc.* **2003**, *755*.
(23) Iyer, P. N.; Smith, A. J. *Acta Crystallogr.* **1967**, *23*, 740.
(24) Amow, G.; Greedan, J. E. *Acta Crystallogr.* **1998**, *C53*, 1053.
(25) Massa, W. *Crystal Structure Determination*; Springer: Berlin, 2004; p 129.
(26) Shannon, R. D.; Prewitt, C. *Acta Crystallogr.* **1970**, *B26*, 1046.
(27) Shannon, R. D. *Acta Crystallogr.* **1976**, *A32*, 751.
(28) Chmaissem, O.; Jorgensen, J. D.; Shaked, H.; Dollar, P.; Tallon, J. L.; *Phys. Rev. B: Solid State* **2000**, *61*, 6401.

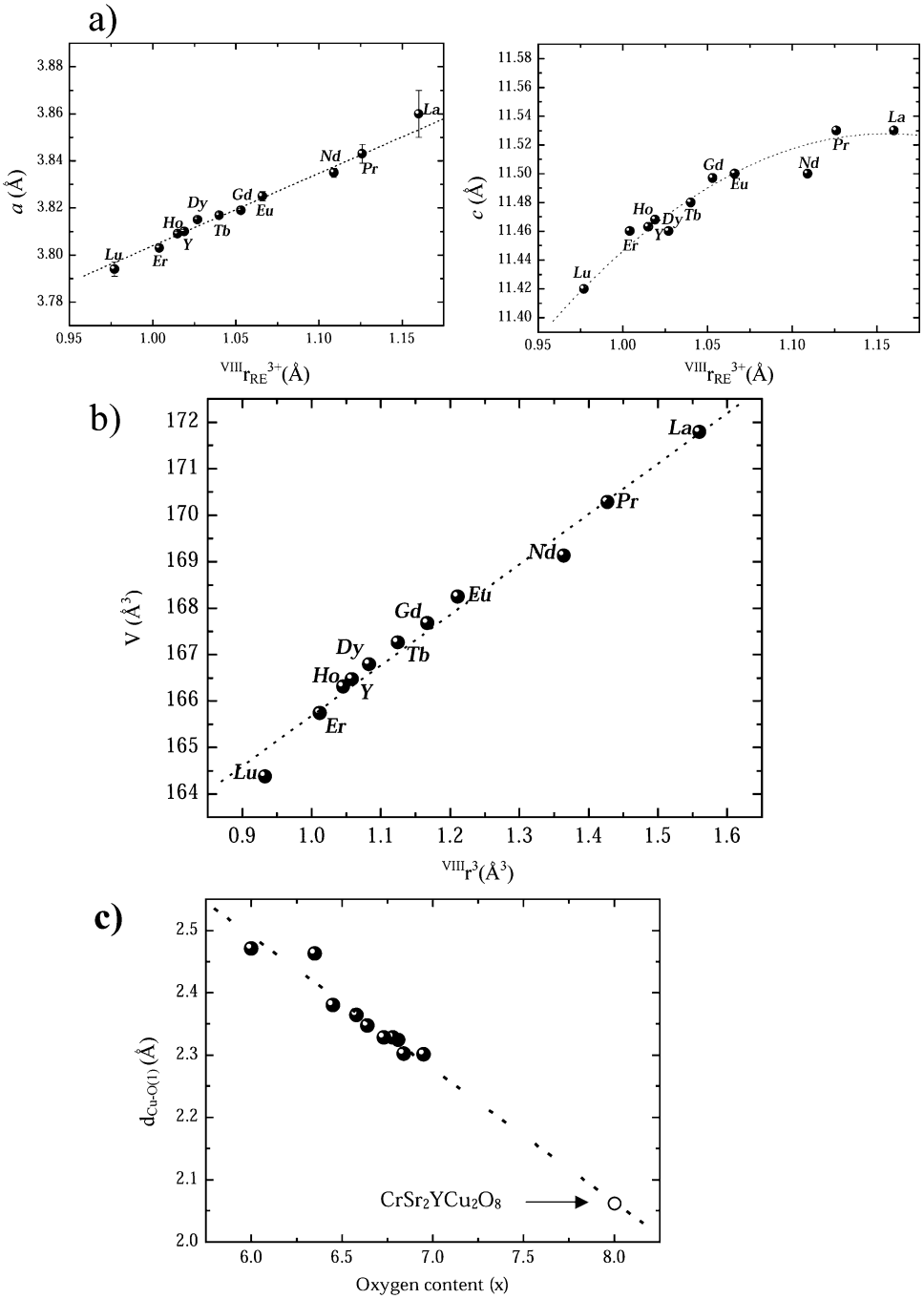

Figure 3. $CrSr_2RECu_2O_8$. (a) Lattice parameters versus the $^{VIII}RE^{3+}$ ionic radii.[25] (b) Unit cell volumes as a function of the cube of the $^{VIII}RE^{3+}$ ionic radii. (c) $d_{Cu-O(1)}$ (Å) distance in $CrSr_2YCu_2O_8$ fitted to the linear relationship between the $d_{Cu-O(1)}$ (Å) distances in Ybco and the oxygen content.[36]

all of the members of the $CrSr_2RECu_2O_8$ family, the equatorial distances are longer than the apical ones; that is, the octahedra are compressed.

If we now consider the average Cr−O distance, it progressively increases with the atomic number of the RE (from 1.890 Å for the La compound to 1.925 Å for the Er one). If one considers a common oxygen ion radius ($r_{O^{2-}} = 1.35$ Å, as suggested by Shannon and Prewitt[26] for two-coordinate oxygen), we can see that the radius of Cr in the octahedra slightly increases along the series (from 0.54 Å for the La compound to 0.575 Å for the Er one). What that means is that, as the rare earth ion size decreases, it attracts more the O(2) oxygen ions, and these carry with them the strontium ions. These will then attract the O(1) oxygen ions, increasing the chromium−oxygen distance. Yet, the average value, 0.56 Å, is quite comparable to the expected radius for Cr^{IV} in an octahedral environment, which is 0.55 Å.[27] On the other hand, Cr^{IV} is a d^2 ion, and therefore, for an octahedral field configuration, $t_{2g}{}^2$, one could expect a Jahn−Teller distortion of the octahedra. Nevertheless, when this happens in the t_{2g} orbital set, as opposed to the e_g one, the distortion is usually rather small, often nonexistent.[29] This is indeed the case for $SrCr^{IV}O_3$, a metallic cubic perovskite, where *regular* octahedra [$d_{Cr-O} = 1.909(2)$ Å] are also

(29) Greenwood, N.; Earnshaw, A. *Chemistry of the Elements*; Pergamon Press: Elmsford, NY, 1984; p 1263.

sharing corners, as in the structure of the present $CrSr_2RECu_2O_8$ family, and the transport properties suggest[30] the electrons being unpaired.

However, when there is a distortion, it can be either an elongation or a flattening of the octahedra. Common wisdom will favor an elongation distortion, because, for the d^2 configuration, there is a more favorable energetic balance.[31] Yet in the dioxide, rutile-type $Cr^{IV}O_2$, where the octahedra share edges, a similar but smaller distortion is observed in the same way as that observed here, with two short apical distances [$d_{Cr-O(1)} = 1.891(2)$ Å] and four long equatorial ones [$d_{Cr-O(3)} = 1.910(2)$ Å; $d_1/d_3 = 0.99$]. Metallic and ferromagnetic properties are shown by CrO_2.[32]

If, indeed, the distortion of the octahedra present in $CrSr_2RECu_2O_8$ is of the Jahn−Teller type, for a d^2 ion in a flattened octahedron, that is, having $d_1/d_3 < 1$, we will have a splitting of the t_{2g} set of the type *one below two*.[33] This will correspond to d_{xy} below and d_{yz} and d_{xz} above (these two orbitals having the same energy). Then, with just two electrons, they will be unpaired (because the pairing energy will be much higher than that of the Jahn−Teller splitting), and one *could* expect, as in CrO_2, interesting electrical and magnetic properties (see below).

It is worth recalling, however, that there are well-known cases where there is an important octahedral distortion that cannot be attributed to a Jahn−Teller effect. Such is the case in, for example, RE_2BaNiO_5, where Ni^{2+} has an electronic configuration $t_{2g}^6e_g^2$ and the [Ni−O_6] octahedra are fairly irregular.[34]

The Copper−Oxygen Polyhedra. In this structure, copper sits in an elongated (here, usually attributed to a Jahn−Teller distortion: Cu^{2+}, $t_{2g}^6e_g^3$), tetragonal pyramid, where the equatorial $d_{Cu-O(2)}$ distances [average 1.915(4) Å] are comparable to those observed in HT_C superconducting cuprates (∼1.88−1.97 Å).[35] However, contrarily to what was observed in the chromium polyhedra, the equatorial copper oxygen distances do not change much with the atomic number of RE. This is a clear indication of the relative stiffness of the $Cu-O_2$ layers in the cuprate structure. On the other hand, the buckling angle,[36] the angle that measures the separation of the copper from the oxygen plane in the [$Cu-O_5$] pyramid, is on the order of 7°, a little higher than that in the ruthenium analogue, where it is 5°. Yet, this is neither a sufficient nor a necessary condition for superconductivity because, for example, the mercury cuprates have flat copper−oxygen planes.[37]

On the other hand, the apical $d_{Cu-O(1)}$ distance, which is substantially longer than the equatorial one, changes quite a bit with the atomic number of RE [from 2.03(4) Å in the La material to 2.11(3) Å in the Er one] but it is, in any event, very short indeed [average 2.06(3) Å]. To our knowledge, this is the shortest apical $d_{Cu-O(1)}$ distance ever observed in this type of Ybco-related material [Ybco = yttrium barium copper oxide; cf. 2.30 Å for Ybco itself (Tc ∼ 95 K), 2.35 Å for $TlSr_2GdCu_2O_7$ (Tc ∼ 110 K), and 2.824 Å for $HgBa_2Cu_2O_7$ (Tc ∼ 125 K), which is the longest one so far observed in these type of solids, which corresponds to the highest Tc for these type of cuprates]. It is worth pointing out that there exists a linear relationship between the oxygen stoichiometry in Ybco and the apical oxygen−basal copper distance, $d_{Cu-O(1)}$, Figure 3c, where the distance observed in $CrSr_2YCu_2O_8$ fits perfectly well.[21] Yet, it should not be deduced in great haste that such a short distance justifies the absence of superconductivity in these chromates, although it could well be related to it. It is pretty obvious that the presence or absence of superconductivity in these (and, indeed, in any) materials will not depend on a single parameter. It would be more appropriate to point to the fact that, because there is no oxygen deficiency in the structure, if we accept the usual oxidation states for the other elements, namely, II for Sr, III for Gd, and IV for Cr, the copper oxidation state will be 2.5+, and it is an observed fact that superconductivity in the cuprates only appears when the formal copper oxidation state is situated in the region ∼2.05−2.25, for hole conductivity.[35] As a matter of fact, in the case of the ruthenates, considering the usual oxidation states of the different ions, that is, $Ru^{V}Sr_2^{II}RE^{III}Cu_2O_8^{-II}$, the copper valence would be Cu^{II}, and no superconductivity should be expected. The fact that these materials are usually considered superconducting is attributed to *self-doping*, that is, *partly* reducing the cation in the CRL and oxidizing the copper in the superconducting planes:

$$Ru^{V} + 2Cu^{II} \leftrightarrow Ru^{V}_{1-x}Ru^{IV}_{x} + 2Cu^{II}_{1-x/2}Cu^{III}_{x/2} \quad (3)$$

which, for $0.1 < x < 0.5$, gives a copper oxidation state within the usual superconducting range (2.05−2.25). Yet, in the case of the present chromates, a similar argument would require a different self-doping "mechanism", that is, *oxidizing the cation* in the CRL in order to partly reduce the copper in the superconducting planes:

$$Cr^{IV} + Cu^{II}Cu^{III} \leftarrow\!\!- \!\!-\!\!\rightarrow Cr^{IV}_{1-x}Cr^{V}_{x} + Cu^{II}_{1+x}Cu^{III}_{1-x} \quad (4)$$

where part of the chromium should go to a *higher* oxidation state Cr^{V}. Actually, for copper in the superconducting range (2.05−2.25), one would require $0.5 < x < 0.9$, which would imply a rather high proportion of the rather infrequent Cr^{V} oxidation state and the coexistence of both Cr^{IV} and Cr^{V} in the same material, something that, as far as we know, there does not yet seem to be an example of in oxide chemistry.

Polyhedral Tilt. Because the chromium−oxygen distances on the *ab* plane [average $d_{Cr-O(3)} = 1.928(3)$ Å] are slightly different from the copper−oxygen ones [average $d_{Cu-O(2)} = 1.915(3)$ Å], the [$Cr-O_6$] octahedra are rotated by 13° around

(30) Chamberland, B. L. *Solid State Commun.* **1967**, *5*(8), 663.
(31) Cotton, F. A.; Wilkinson, G. *Advanced Inorganic Chemistry*, 4th ed.; Wiley & Sons: New York, 1980; p 678.
(32) Goodenough, J. B. *Magnetism and the Chemical Bond*; Wiley & Sons: New York, 1969.
(33) Hoffman, R. D. *Solids and Surfaces*; VCH Publishers: New York, 1988.
(34) Hernández-Velasco, J.; Sáez-Puche, R. *Adv. Mater. Res.* **1994**, *1−2*, 85−82.
(35) Antipov, E. V.; Abukamov, A. M.; Putilin, S. N. *Supercond. Sci. Technol.* **2002**, *15*, R31−R49.
(36) Buchner, B.; Breuer, M.; Freimuth, A.; Freimuth, A.; Kampf, A. P.; *Phys. Rev. Lett.* **1994**, *73*(*13*), 1841.
(37) Balagurov, A. M.; Sheptyakov, D. V.; Aksenov, V. L.; Antipov, E. V.; Putilin, S. N.; Radaelli, P. G.; Marezio, M. *Phys. Rev. B: Solid State* **1999**, *59*(10) 7209.

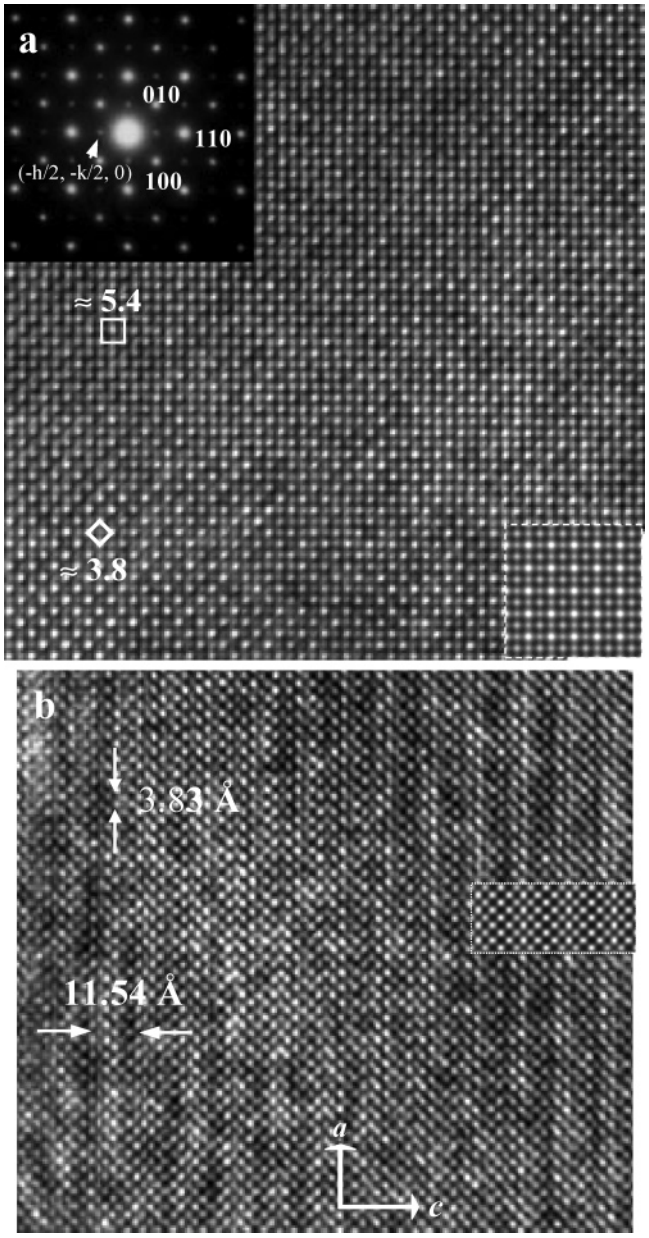

Figure 4. (a) Electron micrograph corresponding to $CrSr_2GdCu_2O_8$, $[001]_p$ zone axis, where both the subcell a_p and the supercell $\sqrt{2}a_p \times \sqrt{2}a_p$ are observed in the image and in the diffraction pattern; the image simulation (Δ*focus*/thickness = −150/75 Å) appears in the inset. (b) $[010]_p$ zone axis, electron micrograph of $CrSr_2GdCu_2O_8$. The calculated image (thickness = 25 Å; defocus = −150 Å) appears in the inset.

the *c* axis, which is the same amount for the corresponding ruthenium octahedra in $RuSr_2GdCu_2O_8$. There is also a tilt of the octahedra that can be inferred from the Cr−O−Cu angle of 168.6°, which is higher than in the case of the equivalent ruthenate,[19] where it is 173.2°. Because of the 4-fold splitting of the O(1) position, this octahedral tilt is randomly distributed around the four possible positions shown in Figure 2.

Microstructure. As discussed above, the powder X-ray diffraction evidence suggests the presence of a tetragonal triple perovskite superstructure, $\sim a_p \times a_p \times 3a_p$, and this can be taken as the *average* crystal structure. However, electron diffraction patterns, as well as the corresponding high-resolution electron micrographs, parts a and b of Figure

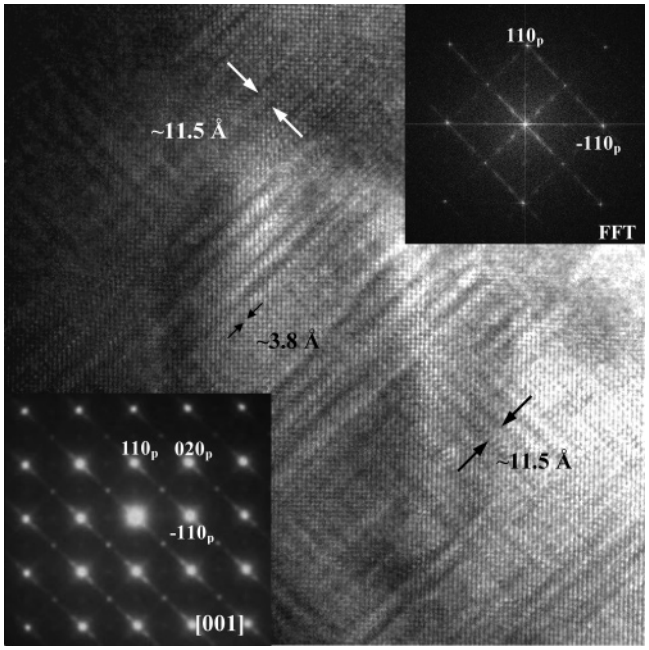

Figure 5. [001] zone axis micrograph showing disordered domains. Both the diffraction pattern and the Fourier Transform show streaking, characteristic of the disorder.

4, clearly show a more complicated situation. Figure 4a shows an electron diffraction pattern and an electron micrograph along the $[001]_p$ zone axis parallel to the same $[001]_s$ axis of the superstructure. The existence of spots at positions h/2, k/2, 0 indicates the presence of a so-called[2] diagonal cell, $\sim a_p\sqrt{2} \times a_p\sqrt{2} \times 3a_p$. Both the basic perovskite cell and the supercell can be distinguished in the figure, upon which a simulated image has been inserted. Figure 4b shows the $[100]_p$ axis parallel to the $[1\bar{1}\ 0]_s$ of the perovskite superstructure of the chromocuprate. Both the simulated and experimental images show the sequence of atom rows expected for the structure of $CrSr_2GdCu_2O_8$. More often than not, however, we could observe the presence of three-dimensional microdomains, Figure 5, in which the orientation of the long $3a_p$ axis changes from domain to domain in one of the three space directions. The electron diffraction pattern shows, besides the ones at positions h/2, k/2, 0 referred to above, which corresponds to the domains having their $c = 3a_p$ axis vertical to the image, other spots at position h/3, k/3, 0, along $[100]_s$ and parallel to $[110]_p$ and $[\bar{1}10]_s$, which are parallel to $[010]_p$. In fact, the image corresponds to a substantial disorder, which is confirmed by the streaking observed both in the electron diffraction pattern (Figure 5 inset, bottom left) and in the Fourier transform of the image (Figure 5 inset, top right). This is, indeed, not unusual in perovskites[3] and perovskite-related materials[39−43] such as $FeCa_2LaFe_2O_8$ and does appear when, in having a

(38) Cava, R. J.; Hewat, A. W.; Hewat, E. A.; Batlogg, B.; Marezio, M.; Rabe, K. M.; Krajewski, J. J.; Peck, W. F., Jr.; Rupp, L. W., Jr. *Physica C* **1990**, *165*(5−6), 419.
(39) Vegas, A.; Vallet-Regí, M.; González-Calbet, J.; Alario-Franco, M. Á. *Acta Crystallogr.* **1986**, *B42*, 167.
(40) Alario- Franco, M. A.; Vallet-Regi, M.; González-Calbet, J. *Cryst. Lattice Defects Amorphous Mater.* **1987**, *16*, 387.
(41) Alario, M. A.; Joubert, J. C.; Levi, J. P. *Mater. Res. Bull.* **1982**, *21*, 733.

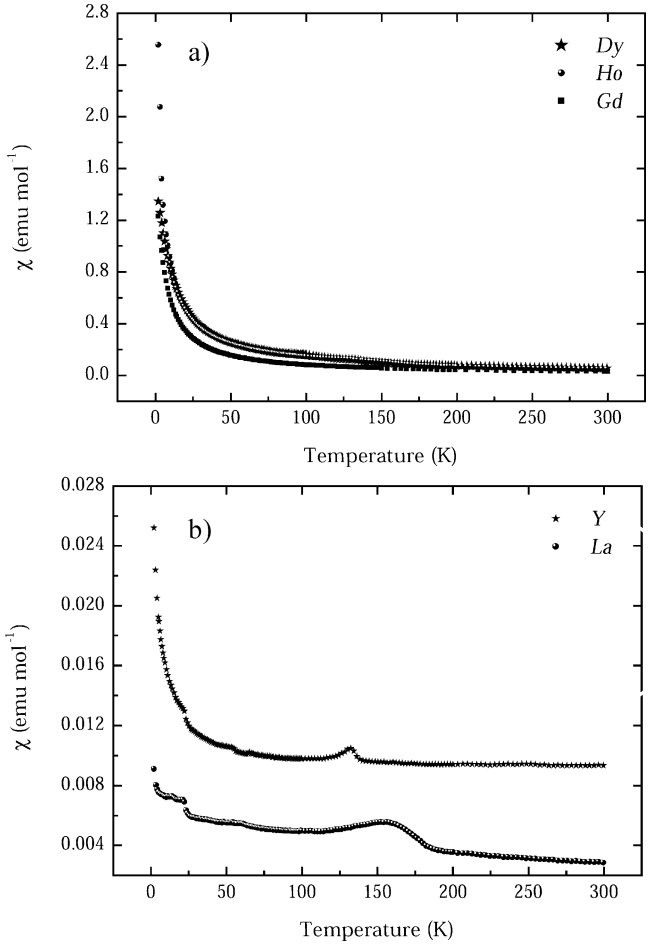

Figure 6. Molar susceptibility as a function of the temperature for the phases with (a) Dy, Ho, and Gd and (b) Y and La.

superstructure, the ratio of the long axis is close to an integer multiple of the basic subcell, that is, in our case, $c/a \approx 3.0$-(1), Table 1. This phenomenon is, in fact, a clear example of three-dimensional intergrowth. It is precisely because of the relatively small size of these domains, obviously below the coherence length of X-ray diffraction (∼110−200 Å[24]), that it requires electron microscopy and diffraction to fully characterize, from the structural point of view, these types of solids. We have recently discussed a similar situation in the ruthenates.[43] Obviously, fitting these domains in the domain walls is a complicated matter that must be facilitated by the splitted O(1) and O(3) positions referred to above.

Magnetic Properties. Preliminary magnetic susceptibility measurements (Figure 6) show two types of behavior, depending upon the magnetic nature of the corresponding rare earth ions. Those with a magnetic moment, such as Dy, Ho, and Gd, Figure 6a, do show a paramagnetic behavior with low susceptibility values that, at moderate temperatures (∼300−100 K), are essentially independent of temperature. This could be an indication of a Pauli paramagnetic behavior and would suggest a somewhat metallic character. However, preliminary electric measurements in the rather small pieces that are obtained in the high-pressure experiments do not show a clearly metallic state. On the other hand, For RE = Y and La, still lower values of the susceptibility are observed and an antiferromagnetic transition is present that peaks at ∼130 K for the Y compound and at ∼150 K for the La one. This seems to be analogous to the magnetic transitions observed in the ruthenates, where they are attributed to an antiferromagnetic state of the Ru ions which, because of the tilt of the octahedra, are slightly canted, giving a low-moment ferromagnetic state[44] that seems compatible with the superconducting properties. The differences in T_N could then be due to differences in the tilt system between both compounds and, indeed, to the different natures of the corresponding cations ($Cr^{IV} = d^2$ and $Ru^{IV-V} = d^{4-3}$).

The absence of the transition signature in the magnetic rare earth ions' cases, Dy, Ho, Gd, and so forth,Figure 6b, will then be due to the influence of the rather high internal field induced by the corresponding RE moments. No superconductivity indications were seen in the magnetic or preliminary electrical data at temperatures down to 4 K.

Conclusions

A new family of materials, $CrSr_2RECu_2O_8$, based on Ybco and having Cr^{IV} in the CRL, has been prepared. These 11 new materials are not superconducting, joining the group of Nb- and Ta-based analogues but opposite that of the isostructural superconducting ruthenates. Nevertheless, they show quite interesting properties. In particular, they share with the ruthenates a remarkable microdomain texture, not seen by X-ray diffraction, characterized by a unit cell $\sim a_p\sqrt{2} \times a_p\sqrt{2} \times 3a_p$. Interestingly enough, these new materials are structurally akin to CrO_2, with which they have in common the flattened octahedral environment of Cr^{IV}. More work is in progress in order to fully characterize the transport and magnetic properties of these interesting compounds.

Acknowledgment. We thank Prof. R. Sáez-Puche (UCM), Prof. J. L. Martínez (ICMM), and Prof. E. Morán (UCM) for valuable comments. We also thank the reviewers for valuable comments. Financial support from Centro de Investigación Cientifica y Tecnológica (Project Mat. 2001-1217), Comunidad Autónoma de Madrid (Projects CAM 007N/0074/2002 and CAM 007N/0074/2003), and the Fundación Areces (Ayudas 2002) is also much appreciated.

IC048929Y

(42) Alario-Franco, M. A.; Henche, M. J. R.; Vallet, M.; Calbet, J. M.; Grenier, J. C.; Wattiaux, A.; Hagenmuller, P. *J. Solid State Chem.* **1983**, *46*, 23−40.
(43) Aguirre, M.; Ruiz-Bustos, R.; Alario-Franco, M. A. *J. Mater. Chem.* **2003**, *13*, 1156−1160.
(44) Lynn, W.; Keimer, B.; Ulrich, C.; Berhard, C.; Tallon, J. L. *Phys. Rev. B: Solid State* **2000**, *61*, 14964.